

Application of Non-uniform Sampling to Three Dimensional Carbon Direct-detection NMR Experiment

Jun-Goo Jee

Research Institute of Pharmaceutical Sciences, College of Pharmacy, Kyungpook National University, Daegu 702-701, Korea
E-mail: jjee@knu.ac.kr

Received July 25, 2011, Accepted August 20, 2011

Key Words : Non-uniform sampling, Carbon direct-detection, Maximum entropy, Multidimensional fourier transformation

In this study, the combined use of 2 new techniques, non-uniform sampling (NUS) and carbon direct-detection (CDD), for the measurement of multidimensional NMR has been demonstrated. NUS is a method for sampling time domain data of indirect dimensions at random sparse points, whereas canonical multidimensional NMR spectra require all the regular grids as sampling points. Of several sparse sampling methods, NUS is advantageous, because it can reduce the errors that originate from the lack of sampling points by randomizing the sampling points. NUS can have denser sampling points at the beginning, where signals decay less than those in the end of sampling, and in turn enhance the signal-to-noise ratio (SNR) in the frequency dimensions per unit time.¹ NUS is applicable to proteins that have been difficult to study using conventional NMR approaches.

CDD is another area where applications have advanced considerably over the last several years.² CDD is an effective technique for detecting NMR signals from proteins that exist under unfavorable conditions to observe or discriminate proton signals, which include paramagnetic proteins, highly deuterated samples, proteins of high salts, and disordered proteins.² Despite the advances in NMR hardware, however, CDD has not been easily employed for practical applications, because the SNR of its result is insufficient. In this paper, NUS and CDD have been used in a combination in a 3D CBCACON experiment,³ expecting the supporting role of NUS in improving the SNR of CDD.

The 3D CBCACON experiment provides the chemical shifts information of $C\alpha/\beta(i-1)-N(i)-C'(i-1)$. The Bruker's default pulse sequence of "c_cbcacn_ia3d" was modified to incorporate the NUS scheme. The sample used in the present study was ubiquitin⁴ (approximately 2.0 mM) and the reference and NUS experiments were performed using a Bruker AV 600 MHz NMR machine equipped with a TCI cryoprobe. The time domains of reference 3D CBCACON data consisted of 256* (F3: $^{13}C'$) \times 28* (F2: ^{15}N) \times 24* (F1: $^{13}C\alpha/\beta$) \times 2 (IPAP) (*means complex point), and the number of transients was 8, leading to the total measurement time of 26 hours. The NUS schedule comprised 270 points, and it corresponded to about 40% of the intact points and required an 11-hour measuring time. As the chemical shifts of the

$^{13}C\alpha/\beta$ atoms evolved under constant time, the points for the $^{13}C\alpha/\beta$ dimension were designed to have equal distribution, whereas the points for ^{15}N dimension distributed to a Gaussian shape with higher density at the beginning (Fig. S1).⁴

To process the NUS data, multidimensional Fourier transformation (MFT)⁵ and the maximum entropy (MaxEnt)⁶ algorithms by using in-house written MFT processing program (J-G. Jee, unpublished data) and the Rowland NMR Toolkit (version 3.0), respectively, were employed. For conventional fast discrete Fourier transformation (FFT) processing and analyses of spectra, NMRPipe software⁷ was used.

The overlaid 2D spectra of [$^{13}C'$, ^{15}N] and [$^{13}C'$, $^{13}C\alpha/\beta$] in FFT, MFT, and MaxEnt results are shown in Figure 1. Because the number of sampling points in the current NUS decreased more than a half, a lower SNR was expected in the results. Although some noise peaks were observed in both the MFT and MaxEnt data due to the lower sensitivity caused by smaller points (Fig. 1), they are tolerable for the backbone chemical shifts assignment. Generally, the spectra reproduced by MaxEnt display a better resolution than those reproduced by MFT. However, insufficient quality or quantity of the input data may alter the chemical shifts. MFT is expected to generate fewer erroneous results despite its

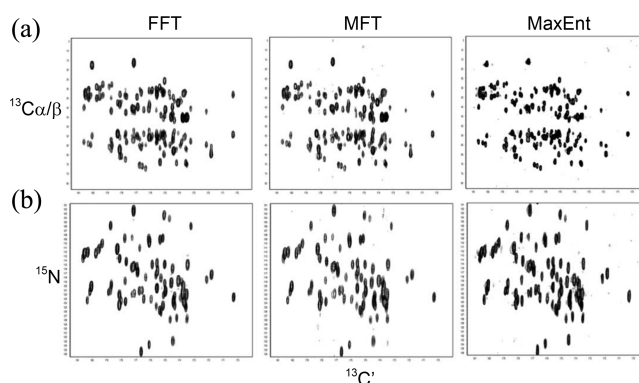


Figure 1. 2D overlay figures of NUS 3D CBCACON in FFT, MFT, and MaxEnt processing. 2D [$^{13}C'$, $^{13}C\alpha/\beta$] overlay (a) and 2D [$^{13}C'$, ^{15}N] overlay (b). All the spectra were drawn with the thresholds whose positions are just above the baseline noise levels for the sensitivity comparison.

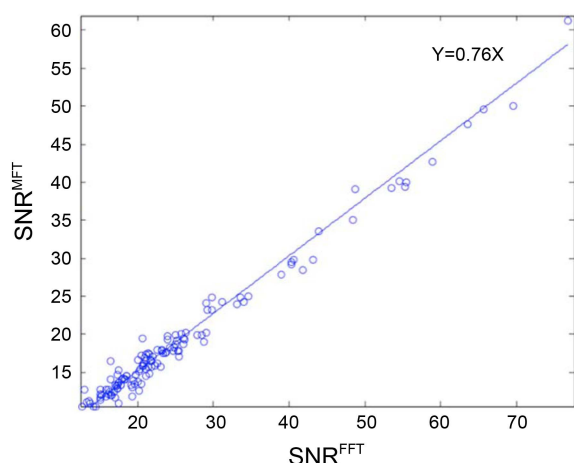


Figure 2. Comparison of signal-to-noise ratio (SNR) in FFT and MFT. X- and Y-axis represent SNR^{FFT} and SNR^{MFT} , respectively. Averaged value of $\text{SNR}^{\text{MFT}}/\text{SNR}^{\text{FFT}}$ is 0.76.

relatively lower SNR, because MFT is the forward method that does not require any fitting parameters. Since the input data are less sensitive in CDD, the poor SNR in MFT and the change of chemical shifts in MaxEnt should be considered. However, the findings of the present study demonstrate that the current NUS 3D CBCACON experiment performed with the concentrated ubiquitin sample does not yield erroneous results, even without gathering data at additional sampling points.

The increment of SNR by NUS was confirmed in the result processed by MFT. If the sensitivity in each sampling point is comparable, the SNR of the resulting spectra gets worse by \sqrt{N} when the number of input data decreases by N times. The value of 0.63 ($=\sqrt{0.4}$) could be expected as $\text{SNR}^{\text{MFT}}/\text{SNR}^{\text{FFT}}$, if the sampling points were omitted in purely random way. However, the actual average value of $\text{SNR}^{\text{MFT}}/\text{SNR}^{\text{FFT}}$ in the peaks was 0.76 (Fig. 2), revealing the increment of SNR by 20% thanks to the weighted NUS schedule. Despite the higher value of $\text{SNR}^{\text{MaxEnt}}/\text{SNR}^{\text{FFT}}$ ($=3.48$ in current data), it was not adequate for the comparison, because $\text{SNR}^{\text{MaxEnt}}$ varies dependent on user input processing parameters of λ and *def*.

Comparison of the peaks in the spectra processed by MFT and MaxEnt reflect the features of MFT and MaxEnt algorithms. I inspected the distributions of differences in linewidth ($\Delta\text{LW}^{\text{MFT/MaxEnt}} = \text{LW}^{\text{MFT/MaxEnt}} - \text{LW}^{\text{FFT}}$) and chemical shift ($\Delta\Omega^{\text{MFT/MaxEnt}} = \Omega^{\text{MFT/MaxEnt}} - \Omega^{\text{FFT}}$) to compare resolution and accuracy in the results (Fig. 3). Most peaks by MaxEnt had negative values in $\Delta\text{LW}^{\text{MaxEnt}}$, meaning better resolutions in MaxEnt. On the other hand, the distribution of $\Delta\Omega^{\text{MaxEnt}}$ was wider than that of $\Delta\Omega^{\text{MFT}}$, which indicates that MFT is more accurate in reproducing chemical shifts. As far as can be ascertained, the data in this study is the first instance wherein more than one method has

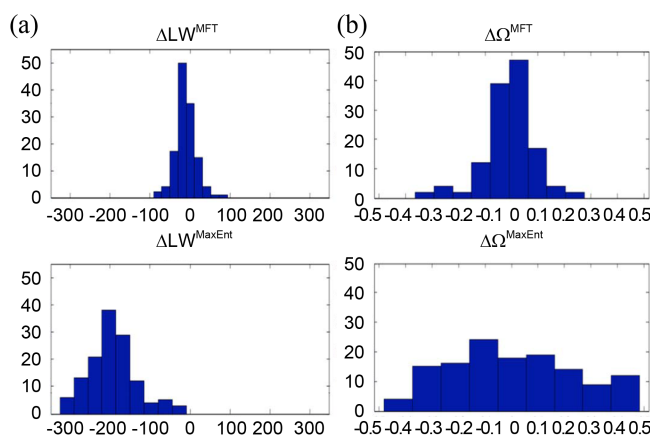


Figure 3. Histogram analysis of the distributions of differences in linewidth ($\Delta\text{LW}^{\text{MFT/MaxEnt}} = \text{LW}^{\text{MFT/MaxEnt}} - \text{LW}^{\text{FFT}}$) (a) and chemical shift ($\Delta\Omega^{\text{MFT/MaxEnt}} = \Omega^{\text{MFT/MaxEnt}} - \Omega^{\text{FFT}}$) (b). Both linewidths and chemical shifts were extracted in $^{13}\text{C}\alpha/\beta$ dimensions.

been employed to process 3D NUS data. Recently an experiment that combined NUS and CDD by another processing method-multidimensional decomposition (MDD)-was reported.⁸ Considering the popularity of MaxEnt, the generality of MFT and the strength of MDD in reproducing the quantitative information, the comparison of the results by MaxEnt, MFT and MDD will be a valuable topic for the future study.

In conclusion, the results prove that NUS and CDD employed in combination can yield favorable results.

Acknowledgments. I am thankful to Drs. Alan Stern and Jeffrey C. Hoch for providing me with the RNMRTK software.

Supporting Information Available. Sampling schedule for NUS 3D CBCACON. This material is available free of charge via the Internet at <http://newjournal.kcsnet.or.kr>.

References

- Rovnyak, D.; Hoch, J. C.; Stern, A. S.; Wagner, G. J. *Biomol. NMR* **2004**, *30*, 1.
- Bermel, W.; Bertini, I.; Felli, I. C.; Piccioli, M.; Pierattelli, R. *Prog. NMR Spectrosc.* **2006**, *48*, 25.
- Bermel, W.; Bertini, I.; Felli, I. C.; Kummerle, R.; Pierattelli, R. *J. Magn. Reson.* **2006**, *178*, 56.
- Jee, J. *Bull. Korean Chem. Soc.* **2008**, *29*, 2017.
- Kazimierczuk, K.; Kozminski, W.; Zhukov, I. *J. Magn. Reson.* **2006**, *179*, 323.
- Stern, A. S.; Li, K. B.; Hoch, J. C. *J. Am. Chem. Soc.* **2002**, *124*, 1982.
- Delaglio, F.; Grzesiek, S.; Vuister, G. W.; Zhu, G.; Pfeifer, J.; Bax, A. *J. Biomol. NMR* **1995**, *6*, 277.
- Bermel, W.; Bertini, I.; Felli, I. C.; Pierattelli, R. *J. Am. Chem. Soc.* **2009**, *131*, 15339.